# Probing the Bonding in Nitrogen-Doped Graphene Using Electron Energy Loss Spectroscopy

**Rebecca J. Nicholls,[†,*] Adrian T. Murdock,[†] Joshua Tsang,[†,§] Jude Britton,[†] Timothy J. Pennycook,[†,‡] Antal Koós,[†] Peter D. Nellist,[†,‡] Nicole Grobert,[†] and Jonathan R. Yates[†]**

[†]Department of Materials, University of Oxford, Parks Road, Oxford OX1 3PH, United Kingdom and [‡]SuperSTEM Laboratory, STFC Daresbury, Keckwick Lane, Warrington WA4 4AD, United Kingdom. [§]Present address: Imperial College London, Exhibition Road, London SW7 2AZ, U.K.

**ABSTRACT** Precise control of graphene properties is an essential step toward the realization of future graphene devices. Defects, such as individual nitrogen atoms, can strongly influence the electronic structure of graphene. Therefore, state-of-the-art characterization techniques, in conjunction with modern modeling tools, are necessary to identify these defects and fully understand the synthesized material. We have directly visualized individual substitutional nitrogen dopant atoms in graphene using scanning transmission electron microscopy and conducted complementary electron energy loss spectroscopy experiments and modeling which demonstrates the influence of the nitrogen atom on the carbon K-edge.

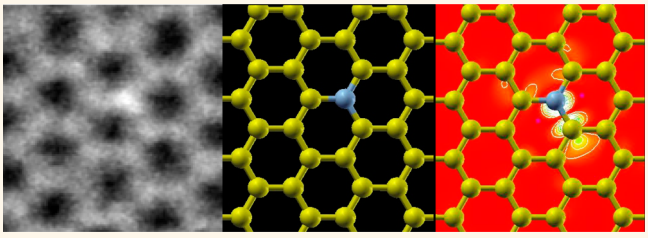

**KEYWORDS:** N-doped · nitrogen doping · CVD graphene · STEM · EELS · modeling

Carbon nanomaterials have a huge variety of potential uses, ranging from sensors[1] to electronics,[1,2] composites,[1,2] drug delivery devices,[2] and many more. The majority of these applications require specific properties, and hence the ability to tailor carbon nanomaterials for a particular use is the goal of extensive research worldwide. Several methods to alter the chemical and physical properties of 1D and 2D carbon nanomaterials have been developed, including the incorporation of heteroatoms such as nitrogen, boron, silicon, and phosphorus.[3,4] Doping graphene and carbon nanotubes with nitrogen is particularly interesting for electrical applications as it can result in *n*-type doping of the carbon material.[5,6] Not all nitrogen defects, however, change the electronic structure in the same way. For example, while substitutional nitrogen defects in single-walled carbon nanotubes result in *n*-type doping, pyridinic nitrogen defects have been predicted to produce *p*-type doping.[7] Recently, it has been shown that the synthesis conditions can affect the way in which nitrogen is incorporated into chemical vapor deposition (CVD) graphene.[8] In addition to this, curvature of the graphene sheets can also affect the relative stability of different defect types.[9] Therefore, different defects are expected to dominate in carbon nanotubes and graphene, and knowledge of exactly how nitrogen atoms are incorporated into the lattice is vital in understanding and optimizing the effect of the doping.

Nitrogen dopant atoms in graphene have been visualized using scanning tunneling microscopy[8,10] and high-resolution transmission electron microscopy,[11,12] but in both cases, image simulations were needed to interpret the images. In this article, we show how the powerful combination of aberration-corrected scanning transmission electron microscopy (STEM) and electron energy loss spectroscopy (EELS) can be used both to identify individual nitrogen atoms incorporated substitutionally within CVD graphene and to probe the resulting changes in the electronic structure. STEM imaging allows the nitrogen atoms to be identified *via* the contrast variation in the images; the intensity of individual atoms is proportional to their atomic number,[13−15] and therefore, images can be interpreted without the need for image simulation. Combining EELS with

* Address correspondence to rebecca.nicholls@materials.ox.ac.uk.

Received for review May 16, 2013 and accepted July 19, 2013.

**Published online July 19, 2013**
**10.1021/nn402489v**

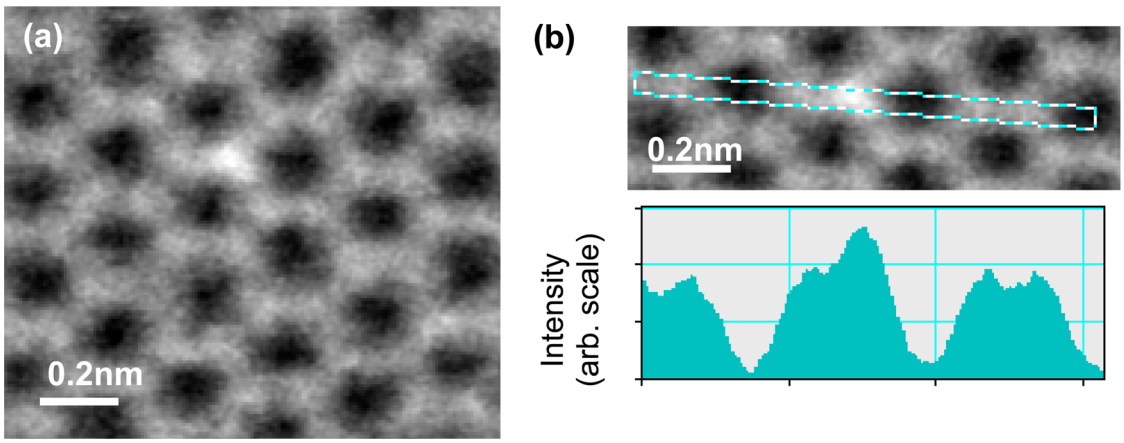


**Figure 1. (a) MAADF image of a single layer of graphene showing a bright dopant atom. (b) Intensity profile showing the increased intensity from the dopant atom.**

STEM enables the simultaneous collection of images and bonding information. This combination of techniques has recently allowed the identification of substitutional silicon atoms in graphene.[16,17] However, recording EELS from a single nitrogen dopant is a significantly greater challenge due to the much smaller cross section of the nitrogen K-edge as compared to the silicon L-edge, and although it may be possible to detect the nitrogen K-edge,[18] resolving the fine structure is very difficult. Instead, we show that the effect of the nitrogen on the neighboring carbon atoms results in a measurable change in the carbon K-edge EELS fine structure. As there are three neighboring carbon atoms for each single substitutional nitrogen atom, and the cross section for scattering from carbon is higher than for nitrogen, the change in the carbon K-edge is more easily observed than the presence of the nitrogen K-edge fine structure. First-principles calculations are used to directly relate the changes in the observed EELS spectra to the C−N bond. This method provides a way of probing the electronic structure without needing to obtain EELS fine structure information from the dopant atoms itself and could be applied to other dopant atoms with EELS edges that are difficult to observe.

## RESULTS AND DISCUSSION

STEM was used to look for evidence of nitrogen atoms in the nitrogen-containing CVD graphene (N-graphene) sample. Figure 1 shows a medium-angle annular dark-field (MAADF) image with a brighter dopant atom within the graphene lattice. The image was processed using a filter as described in ref 19, but the bright atom can also be seen in the raw image (see Supporting Information). The intensity variation is due to Rutherford scattering from the partially screened atomic nucleus and should increase with atomic number as $Z^{\nu}$ where $\nu$ is expected to be in the range 1.5−1.8. Statistical analysis of the intensity ratio of the bright atom to the carbon atoms gives a value of 1.3:1 (see Supporting Information), which, by comparison with the work of Krivanek *et al.*,[19] identifies the dopant atom as being nitrogen.

The nitrogen atom in Figure 1 has replaced a carbon atom within the graphene lattice. Indeed, we found that all the dopant atoms observed in this study occurred as substitutional defects. This is in agreement with a recent STM study on CVD nitrogen-doped graphene produced under similar synthesis conditions.[10]

We recorded EELS spectra to examine the effect of the dopant on the electronic structure of the surrounding carbon atoms. A predefined region around a dopant atom was repeatedly scanned to acquire EELS spectra (for instance, the red box in Figure 2a). Monitoring the MAADF image of this region during the EELS acquisition enabled us to counteract any sample drift and ensure that the nitrogen atom remained centered in the scanned area. Several exposures were acquired and summed to reduce the noise in the EELS measurements. By comparing the EELS spectra taken from the region surrounding a nitrogen dopant with that from pristine graphene, we can see that the nitrogen does influence the carbon K-edge (Figure 2b). The primary change is an extra feature at ∼290 eV. While this change is quite subtle, it is reproducible and was seen for all the dopant atoms studied (see Supporting Information). There are two sharp peaks in the spectra at ∼297 and 302 eV which must be associated with a particular channel on the CCD as we found that they did not move when the drift tube was changed. This indicates that they are not real features and are most likely due to bad pixels. It is important to note that despite recording the energy range containing the nitrogen K-edge we found that this feature was not visible in our spectra. This can be ascribed to a combination of two factors; first, there are fewer nitrogen atoms than carbon atoms present in the scanned region, and second, the cross section for nitrogen is smaller than that for carbon by a factor of ∼2. The combination of these two factors means that the nitrogen K-edge is expected to be ∼20 times smaller

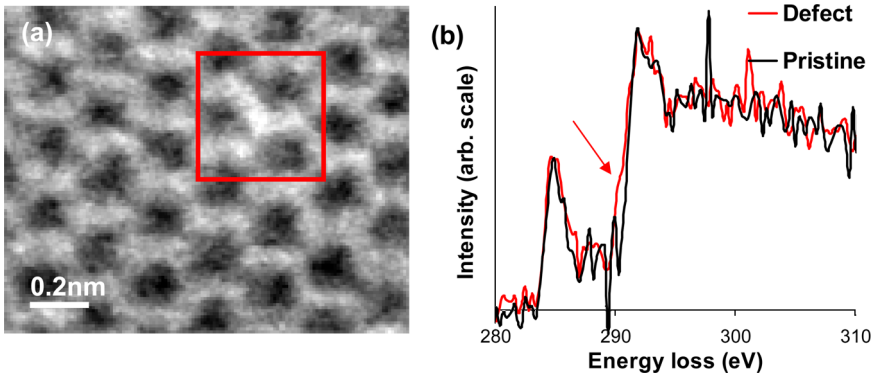


**Figure 2. (a) Processed MAADF image of a dopant atom in graphene. (b) Carbon K-edges obtained from the region (outlined by a box) surrounding the dopant atom shown in (a) and from a region of pristine graphene. (The peaks in the spectra at ~297 and 302 eV are artifacts and are likely to be due to bad pixels on the CCD camera.)**

than the carbon K-edge and would not be expected to be visible above the noise.

In order to understand the observed changes in the EELS spectra from the defect region, we used first-principles quantum mechanical simulations using a plane-wave pseudopotential density functional theory code (CASTEP)[20] together with the OptaDOS spectral simulation code.[21] We simulated EELS spectra for the three symmetrically unique atoms closest to the nitrogen dopant (Figure 3) and for pristine graphene. The EELS spectrum of pristine graphene shows a $\pi^*$ peak at ~1 eV and a $\sigma^*$ peak at ~8 eV above the edge onset. By comparison, the spectrum from the carbon atom directly bonded to the nitrogen (C1) has an additional peak at ~4.5 eV above the edge onset (Figure 4). Spectra from carbon atoms further away from the nitrogen atom do not feature this additional peak and more closely resemble pristine graphene; however, the next nearest neighbor carbon (C2) has a noticeably earlier onset to its $\sigma^*$ peak.

To understand the origins of the additional peak, we examine the site-projected partial density of states (p-DOS) as within our dipole approximation only states with p-like character will contribute toward the spectrum. As expected, the p-DOS from atom C1 (Figure 4b) has a peak at ~4.6 eV corresponding to the extra peak in the EELS spectrum simulated from this atom. Visualization of these states (Figure 5) shows that they are concentrated around the nitrogen defect and the atom C1. The inclusion of the core hole in the simulation is crucial as without it the extra peak in the spectrum is smaller and higher in energy, making it much more difficult to distinguish from the $\sigma^*$ peak at ~8 eV. The states visualized in Figure 5 hence arise from the interaction of the nitrogen atom and the core hole on the carbon atom. The alignment of these states along the C−N bond manifests itself in the orientation dependence of the simulated spectra; the peak is only present when there is a contribution from the momentum transfer (**q**) associated with the beam electron along the C−N bond (see Supporting Information).

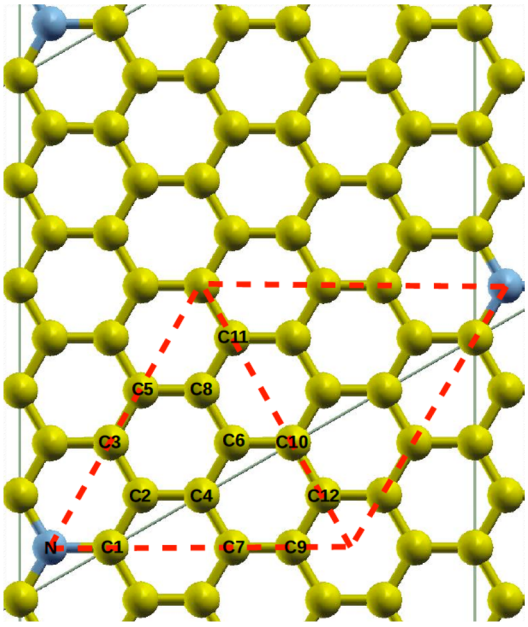


**Figure 3. Graphene lattice containing substitutional nitrogen atoms with the unit cell marked in solid (gray) lines and the symmetrically unique atoms labeled according to their distance form the nitrogen dopant atoms. The dashed (red) lines provide a guide for the eye.**

Extra peaks are also present in the p-DOS from atom C2 and, as they are at higher energies (5.4 and 6.1 eV) and not as sharp, these peaks are responsible for the less sharp onset seen in the EELS spectrum simulated from this atom. The p-DOS for atom C3 does not contain any extra peaks in this region.

The measured EELS spectrum (Figure 2b) contains contributions from approximately 11 atoms surrounding the nitrogen dopant, only three of which are directly bonded to the nitrogen atom. In order to compare the simulated data with experiment, we combine the computed EELS spectra from atoms C1, C2, and C3 in the ratio 3:6:2, consistent with the scanned area outline by a red box in Figure 2a. The feature at ~5 eV above the edge onset is still present in the combined spectrum (Figure 6), but the prominence of the feature in the

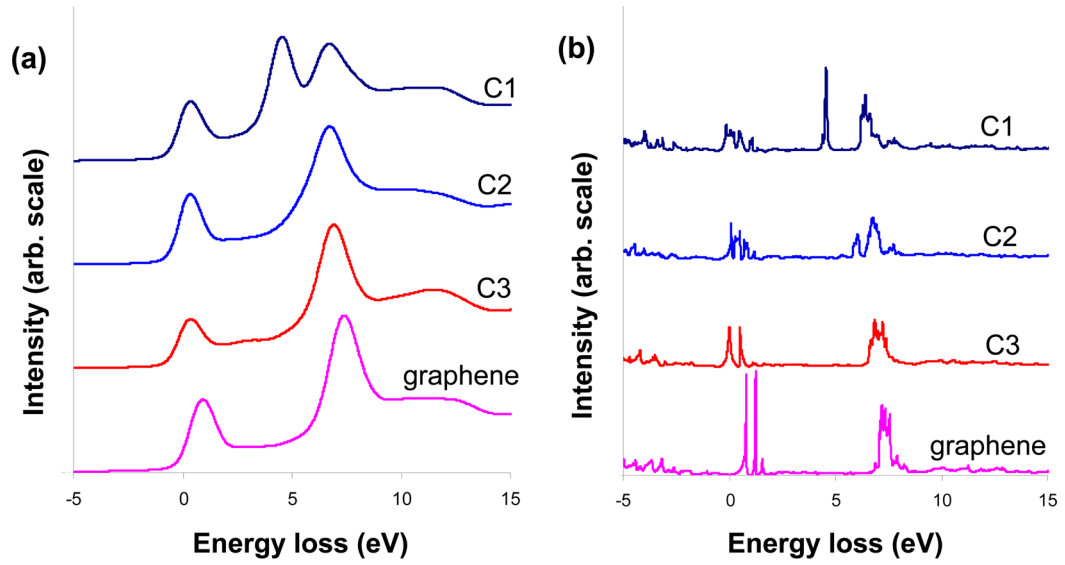


**Figure 4. Simulated EELS spectra (a) and p-DOS (b) from pristine graphene and atoms C1, C2, and C3.**

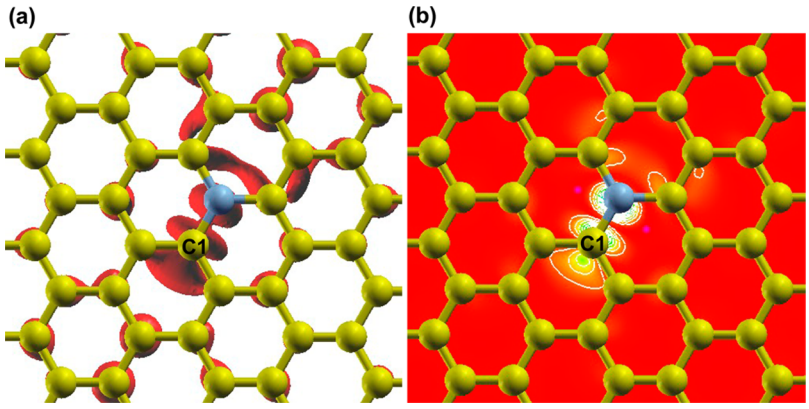


**Figure 5. (a) Isosurface of the charge density (constructed using the wave functions at the gamma point) of the bands which contribute to the peak at ~4.6 eV in the C1 p-DOS (isosurface value 0.03 e/Å$^3$). (b) Variation of the charge density distribution in the plane of the atoms.**

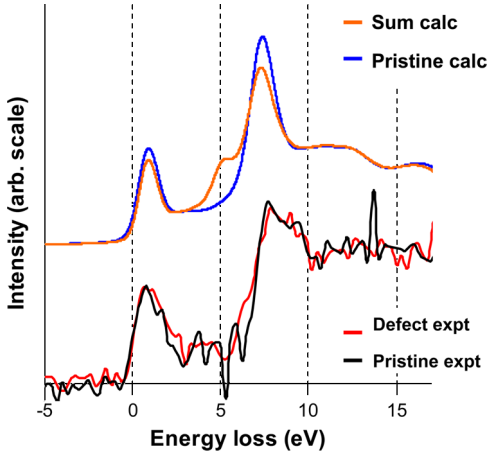


**Figure 6. Experimental and modeled EELS spectra from pristine and defect regions.**

spectrum has been reduced by the addition of the spectra from atoms C2 and C3. Our simulations show an isotropically averaged spectrum; however, we expect that the observed spectrum will correspond to a range of momentum transfer directions which differ from an isotropic average. The distribution will change the ratio of the peak heights, but withstanding this, we can clearly identify the additional feature in the defect region EELS spectrum as resulting from the C—N bond.

## CONCLUSION

In summary, substitutional nitrogen defects in CVD graphene have been visualized using contrast variation in STEM without the need for image simulations. Simultaneous recording of the EELS spectra has provided complementary bonding information, and there is a change in the carbon K-edge from the region surrounding the nitrogen dopant atom compared to pristine graphene. Modeling shows that the change in the carbon K-edge near to the nitrogen defect is due to the influence of the nitrogen atom on the electronic structure of the neighboring carbon atoms, and the extra feature can be attributed to the C—N bonds.

The combination of the larger cross section for carbon, compared to nitrogen, and the fact that there are three neighboring carbon atoms for one nitrogen defect means that it is possible to see the change in the carbon K-edge even though the nitrogen K-edge was not detected. Using the change in electronic structure on the surrounding carbon atoms has been shown to be a useful way of probing the electronic structure of a dopant defect when the EELS edge of the dopant atom itself is difficult to detect. Doping offers the potential to tailor the properties of graphene and carbon nanotubes for a myriad of applications, such as sensors and electronics. Characterization methods such as those demonstrated here are essential to fulfilling this potential because they allow us to fully understand and optimize the effect of doping.

## MATERIALS AND METHODS

We synthesized CVD N-graphene from nitrogen-containing precursors. Further details of the synthesis can be found in the Supporting Information. A TEM sample was then prepared using a method similar to that described by Regan *et al.*[22] but with ammonium persulfate used as the copper substrate etchant.

STEM imaging and EELS measurements were carried out using an aberration-corrected Nion UltraSTEM 100, operated at 60 kV to minimize knock-on damage caused by the electron beam.[11,23,24] The UltraSTEM is equipped with a cold field emission electron source, a corrector capable of neutralizing up to fifth order aberrations,[25] and an Enfina EEL spectrometer. For imaging, we used the medium-angle annular dark-field (MAADF) mode (with inner and outer detector angles of 41.1 and 195 mrad) as this mode has been successfully used by Krivanek *et al.*[19] to identify carbon and oxygen atoms incorporated substitutionally within a boron nitride sheet.

In order to model the EELS spectra, we used a periodic model of nitrogen-substituted graphene in which the nitrogen defects were separated by ~12 Å (a 5 × 5 × 1 supercell). Geometry optimization of this model produced a C−N bond length $1 \times 10^{-2}$ Å shorter than that of the C−C bond in pristine graphene, a lattice distortion too small to be observed in the present MAADF images.[19] The core hole was included in the EELS simulations by constructing a pseudopotential with an electron removed from the 1s orbital. We carefully checked that the spectra reported in Figure 4 did not change when any of the numerical criteria controlling the simulation were increased (*e.g.*, basis set size, Brillouin zone sampling, supercell size). Further details of the calculations can be found in the Supporting Information.

*Conflict of Interest:* The authors declare no competing financial interest.

*Acknowledgment.* The authors would like to thank Aleksey Shmeliov for his help with processing the raw MAADF images, and Lewys Jones for producing the integrated intensity data using Absolute Integrator v1.1.5. We are grateful to the Engineering and Physical Sciences Research Council (Grant EP/H046550/1 and EPSRC Pathways to Impact Awards), The Royal Society, the European Research Council (ERC) Starting Grant (ERC-2009-StG-240500 DEDIGROWTH; and ERC-2012-PoC 309786 DEVICE), the Commonwealth Scholarship Commission and the University of Oxford Clarendon Fund for financial support. STEM experiments were performed at SuperSTEM, the EPSRC UK national facility for aberration-corrected STEM.

*Supporting Information Available:* Details of the graphene synthesis, the raw image used to produce Figure 1a, information on the reproducibility of the defect spectrum, and further computational details and orientation dependence of the spectrum. This material is available free of charge *via* the Internet at http://pubs.acs.org.

## REFERENCES AND NOTES

1. Novoselev, K. S.; Fal'ko, V. I.; Colombo, L.; Gellert, P. R.; Schwab, M. G.; Kim, K. A Roadmap for Graphene. *Nature* **2012**, *490*, 192–200.
2. Hirsch, A. Functionalization of Fullerenes and Carbon Nanotubes. *Phys. Status Solidi B* **2006**, *243*, 3209–3212.
3. Koós, A.; Dillon, F.; Obraztsova, E. A.; Crossley, A.; Grobert, N. Comparison of Structural Changes in Nitrogen and Boron-Doped Multi-walled Carbon Nanotubes. *Carbon* **2010**, *48*, 3033–3041.
4. Koós, A.; Nicholls, R. J.; Dillon, F.; Kertész, K.; Biró, L. P.; Crossley, A.; Grobert, N. Tailoring Gas Sensing Properties of Multi-walled Carbon Nanotubes by *In Situ* Modification with Si, P and N. *Carbon* **2012**, *50*, 2816–2834.
5. Terrones, M.; Jorio, A.; Endo, M.; Rao, A. M.; Kim, Y. A.; Hayashi, T.; Terrones, H.; Charlier, J.-C.; Dresselhaus, G.; Dresselhaus, M. S. New Directions in Nanotube Science. *Mater. Today* **2004**, *7*, 30–45.
6. Wang, H.; Maiyalagan, T.; Wang, X. Review on Recent Progress in Nitrogen-Doped Graphene: Synthesis, Characterization, and Its Potential Applications. *ACS Catal.* **2012**, *2*, 781–794.
7. Cruz-Silva, E.; López-Urías, F.; Muñoz-Sandoval, E.; Sumpter, B. G.; Terrones, H.; Charlier, J.-C.; Meunier, V.; Terrones, M. Electronic Transport and Mechanical Properties of Phosphorus- and Phosphorus−Nitrogen-Doped Carbon Nanotubes. *ACS Nano* **2009**, *3*, 1913–1921.
8. Lv, R.; Li, Q.; Botello-Méndez, A. R.; Hayashi, T.; Wang, B.; Berkdemir, A.; Hao, Q.; Elías, A. L.; Cruz-Silva, R.; Gutiérrez, H. R.; *et al.* Nitrogen-Doped Graphene: Beyond Single Substitution and Enhanced Molecular Sensing. *Sci. Rep.* **2012**, *2*, 586-1-8.
9. Yang, S. H.; Shin, W. H.; Kang, J. K. The Nature of Graphite- and Pyridinelike Nitrogen Configurations in Carbon Nitride Nanotubes: Dependence on Diameter and Helicity. *Small* **2008**, *4*, 437–441.
10. Zhao, L.; He, R.; Taeg Rim, K.; Schiros, T.; Soo Kim, K.; Zhou, H.; Gutiérrez, C.; Chockalingam, S. P.; Arguello, C. J.; Pálová, L.; *et al.* Visualizing Individual Nitrogen Dopants in Monolayer Graphene. *Science* **2011**, *333*, 999–1003.
11. Susi, T.; Kotakoshi, J.; Arenal, R.; Kurasch, S.; Jiang, H.; Skakalova, V.; Stephan, O.; Krasheninnikov, A. V.; Kauppinen, E. I.; Kaiser, U.; *et al.* Atomistic Description of Electron Beam Damage in Nitrogen-Doped Graphene and Single-Walled Carbon Nanotubes. *ACS Nano* **2012**, *6*, 8837–8846.
12. Mayer, J. C.; Kurasch, S.; Park, H. J.; Skakalova, V.; Künzel, D.; Gross, A.; Chuvilin, A.; Algara-Siler, G.; Roth, S.; Iwasaki, T.; *et al.* Experimental Analysis of Charge Redistribution Due to Chemical Bonding by High-Resolution Transmission Electron Microscopy. *Nat. Mater.* **2011**, *10*, 209–215.
13. Crewe, A. V.; Wall, J.; Langmore, J. Visibility of Single Atoms. *Science* **1970**, *168*, 1338–1340.
14. Nellist, P. D.; Pennycook, S. J. Direct Imaging of the Atomic configuration of Ultra-dispersed Catalysts. *Science* **1996**, *274*, 413–415.
15. Nicholls, R. J.; Sader, K.; Warner, J. H.; Plant, S. R.; Porfyrakis, K.; Nellist, P. D.; Briggs, G. A. D.; Cockayne, D. J. H. Direct Imaging and Chemical Identification of the Encapsulated Metal Atoms in Bimetallic Endofullerene Peapods. *ACS Nano* **2010**, *4*, 3943–3948.
16. Ramasse, Q. M.; Seabourne, C. R.; Kepaptsoglou, D. M.; Zan, R.; Bangert, U.; Scott, A. Probing the Bonding and Electronic Structure of Single Atom Dopants in Graphene with Electron Energy Loss Spectroscopy. *Nano Lett.* **2013**, 10.1021/nl304187e.

17. Zhou, W.; Kapetanakis, M. D.; Prange, M. P.; Pantelides, S. T.; Pennycook, S. J.; Idrobo, J.-C. Direct Determination of the Chemical Bonding of Individual Impurities in Graphene. *Phys. Rev. Lett.* **2012**, *109*, 206803-1-5.
18. Suenaga, K.; Akiyama-Hasegawa, K.; Niimi, Y.; Kobayashi, H.; Nakamura, M.; Liu, Z.; Sato, Y.; Koshino, M.; Iijima, S. Atomic Imaging and Spectroscopy of Low-Dimensional Materials with Interrupted Periodicities. *J. Electron Microsc.* **2012**, *61*, 285–291.
19. Krivanek, O. L.; Chisholm, M. F.; Nicolosi, V.; Pennycook, T. J.; Corbin, G. J.; Dellby, N.; Murfitt, M. F.; Own, C. S.; Szilagyi, Z. S.; Oxley, M. P.; *et al.* Atom-by-Atom Structural and Chemical Analysis by Annular Dark-Field Electron Microscopy. *Nature* **2010**, *464*, 571–574.
20. Clark, S. J.; Segall, M. D.; Pickard, C. J.; Hasnip, P. J.; Probert, M. J.; Refson, K.; Payne, M. C. First Principles Methods Using CASTEP. *Z. Kristallogr.* **2005**, *220*, 567–570.
21. Nicholls, R. J.; Morris, A. J.; Pickard, C. J.; Yates, J. R. OptaDOS—A New Tool for EELS Calculations. *J. Phys.: Conf. Ser.* **2012**, *371*, 012062-1-4.
22. Regan, W.; Alem, N.; Alemán, B.; Geng, B.; Girit, C.; Maserati, L.; Weng, F.; Crommie, M.; Zettl, A. A Direct Transfer of Layer-Area Graphene. *Appl. Phys. Lett.* **2010**, *96*, 113102-1-3.
23. Smith, B. W.; Luzzi, D. E. Electron Irradiation Effects in Single Wall Carbon Nanotubes. *J. Appl. Phys.* **2001**, *90*, 3509–3515.
24. Krivanek, O. L.; Dellby, N.; Murfitt, M. F.; Chisholm, M. F.; Pennycook, T. P.; Suenaga, K.; Nicolosi, V. Gentle STEM: ADF Imaging and EELS at Low Primary Energies. *Ultramicroscopy* **2010**, *110*, 935–945.
25. Krivanek, O. L.; Corbin, G. J.; Dellby, N.; Elston, B. F.; Keyse, R. J.; Murfitt, M. F.; Own, C. S.; Szilagyi, Z. S.; Woodruff, J. W. An Electron Microscope for the Aberration-Corrected Era. *Ultramicroscopy* **2008**, *108*, 179–195.